Applied Catalysis B: Environmental 90 (2009) 478–484

Contents lists available at ScienceDirect

Applied Catalysis B: Environmental

journal homepage: www.elsevier.com/locate/apcatb

Structure sensitivity of dimethylamine deep oxidation over Pt/Al_2O_3 catalysts

B. Grbic [a], N. Radic [a,*], Z. Arsenijevic [a], R. Garic-Grulovic [a], Z. Grbavcic [b]

[a] Institute for Chemistry, Technology and Metallurgy, Department of Catalysis and Chemical Engineering, University of Belgrade, Njegoseva 12, Belgrade, Serbia
[b] Faculty of Technology and Metallurgy, University of Belgrade, Karnegijeva 4, Belgrade, Serbia

ARTICLE INFO

Article history:
Received 30 January 2009
Received in revised form 31 March 2009
Accepted 4 April 2009
Available online 11 April 2009

Keywords:
Pt/Al_2O_3 catalyst
Deep oxidation
Dimethylamine
Kinetics
Structure sensitivity

ABSTRACT

The deep oxidation of dimethylamine (DMA) was studied over Pt/Al_2O_3 catalysts with small (1 nm) and large (7.8–15.5 nm) Pt crystallite sizes. The turnover frequency (TOF) was higher for the large than for the small Pt crystallites, indicating that the reaction is structure sensitive. Two kinetic models were used to interpret the obtained results, i.e., the Mars van Krevelen and a mechanism based on the adsorption of oxygen and adsorption of dimethylamine on different active sites were employed. Both models showed that the activation energy for the oxygen chemisorption rate constant (k_o) decreased with increasing of Pt crystallite size and that the activation energy for the surface reaction rate constant (k_i) was independent of the Pt crystallite size. The structure sensitivity may be explained by differences in the reactivity of the oxygen adsorbed on these Pt crystallites.

The Mars van Krevelen model fits the TOF values very well at concentrations of DMA higher than 1500 ppm, while in the lower concentrations region, the model under predicts the experimental data. The model based on the adsorption of oxygen and DMA on different active sites fits the experimental data quite well over the whole temperature and concentration range. The fitted values of the Henry adsorption constant are independent of the Pt crystallite size.

1. Introduction

Deep catalytic oxidation of volatile organic compounds (VOCs) on noble metals is a widely used method to remove VOCs from industrial waste gases, especially in processes with high flow rates of waste gases and low concentrations of VOCs [1,2]. Typical catalysts for deep oxidation of VOCs are based on precious metals. As a general rule, any surface reaction over a supported metal catalyst the rate of which is affected by a change in the metal particle size is considered to be structure sensitive [3]. Several studies have reported that the intrinsic rate of the deep oxidation of VOCs over supported platinum and palladium catalysts are dependent on the particle size, i.e., the specific activity (activity per exposed metal atom) of supported noble metal is influenced by the metal crystallite size [4–10]. There are numerous papers indicating that the strength of the oxygen adsorption plays a key role in the observed structure sensitivity of these reactions [11–18]. In addition, some authors interpret the structure sensitivity of the deep oxidation of VOCs considering the adsorption of hydrocarbons as the rate-determining step and the readiness of the rupture of the weakest C–H bonds is affected by the metal crystallite size [19–21]. However, there is agreement that changes in the specific activity can be attributed to morphological effects rather than to the chemical state.

An understanding of the root causes of structure sensitivity is an important challenge, both for the fundamental study or practical use of catalysts. The structure sensitivity can be clearly evidenced and well explained using a detailed determination of the kinetic parameters, such as activation energy for each elementary step of the oxidation of VOCs, for catalysts with different Pt particle sizes. The results of a previous study [11] of the kinetics of toluene and *n*-hexane oxidation over Pt/Al_2O_3 catalysts with platinum mean crystallite sizes ranging from 1.0 to 15.5 nm showed that both the kinetic parameters and the turnover frequency are affected by the mean crystallite size of the platinum. The structure sensitivity was explained by differences in the reactivity of the adsorbed oxygen on small and large Pt crystallites.

Within this work, the kinetics of the deep oxidation of dimethylamine (DMA) over Pt/Al_2O_3 catalysts with different platinum mean crystallite size, small and large, was investigated. Reactions of DMA are an important commercial route for the production of several formulations of herbicides, which have wide-ranging applications as agrochemicals. The vapours of both the reactants and products are potentially hazardous for the environment. Consequently, the working objective of this study was to estimate the feasibility of employing a Pt/Al_2O_3 catalyst for DMA removal. However, the products of the catalytic oxidation of DMA

* Corresponding author. Tel.: +381 11 2630 213; fax: +381 11 2637 977.
E-mail address: nradic@nanosys.ihtm.bg.ac.rs (N. Radic).

0926-3373/$ – see front matter © 2009 Elsevier B.V. All rights reserved.
doi:10.1016/j.apcatb.2009.04.008

over a Pt/Al_2O_3 catalyst include NO*x*, in addition to the benign products CO_2 and H_2O, which certainly requires additional treatment; i.e., selective catalytic reduction, adequate NO*x* storage devices, etc.

2. Experimental

2.1. Catalysts preparation

The catalysts were synthesized by impregnation of a ($\gamma+\theta$) Al_2O_3 support (Rhone-Poulenc, Type 531A, in the form of spheres with a diameter of 3.0 ± 0.3 mm) using an aqueous solution of hexachloroplatinic acid. Briefly, the support was dried for 4 h at 120 °C. An adequate amount of an aqueous solution of hexachloroplatinic acid was added to the support (about 5 $cm^3\ g^{-1}$ support) by the incipient wetness method. The concentration of hexachloroplatinic acid in the impregnating solution was 1×10^{-2} mol/l. The duration of the impregnation of the support was 3 min. After adsorption of hexachloroplatinic acid, the catalyst was filtered, rinsed with distilled water to avoid the negative reaction of chloride ions and air-dried at 110 °C for 2 h. The catalyst was reduced in a dynamic hydrogen-nitrogen mixture. The temperature was increased to 500 °C at a programmed and maintained at this temperature for 5 h, whereby the catalyst was reduced. The platinum loading determined by chemical analysis was 0.12 wt.%. The catalysts had an egg-shell distribution, with almost all platinum content deposited in the outer shell of the support to a depth of 100 μm. The surface area of the sample prepared by the above procedure was 110 $m^2\ g^{-1}$. In order to affect the Pt particle size, the catalyst synthesized in the previous procedure was calcinated in air at 700 °C for 48 h. The sintered sample was then reduced under the same conditions as the fresh sample. The sintered catalyst had a surface area of 100 $m^2\ g^{-1}$. Since the contribution of Pt to the overall specific surface area is negligible (less than 1 $m^2\ g^{-1}$), the decrease in the specific surface area by about 10% should be ascribed solely to the support sintering. More specifically, this is the consequence of the partial disappearance of pores of size about 2–4 nm [22].

2.2. Catalysts characterization

The platinum dispersion measurements were performed by CO chemisorption at a temperature of 24 ± 0.2 °C using a pulse gas chromatographic method, a self-made apparatus equipped with a TCD detector of a Varian Aerograph model 920 gas chromatograph. Before the chemisorption measurements, the catalyst samples were treated at 450 °C in a helium flow for 1 h. After cooling to room temperature, the CO was pulsed (pulse volume 0.1 cm^3) into the helium stream (30 cm^3/min) through an adsorption cell. The catalyst adsorbed the CO pulses until saturation and the fraction of CO not adsorbed was detected by a thermal conductivity detector (TCD).

The specific surface area measurements were performed by nitrogen adsorption at −196 °C, using the same apparatus as employed in the CO chemisorption measurements. Before the measurements, the samples were treated at 450 °C in a helium flow for 2 h. After that, a gas mixture of 27 vol.% of nitrogen in helium (30 cm^3/min) was passed over the sample and the sample cell was cooled by immersion in liquid nitrogen. The cooled sample adsorbs a certain amount of nitrogen from the gas stream and the adsorption equilibrium was established. When the liquid nitrogen bath was removed, the sample warmed and the adsorbed nitrogen was released, enriching the effluent which was monitored by a TCD detector. The specific surface areas of the samples were calculated by the "one point" BET method in a manner similar to that used in a standard volumetric BET method.

2.3. Kinetic measurements

The kinetics experiments of DMA oxidation were performed in a fixed bed catalytic reactor made of a stainless steel tube having 6 mm o.d., 4 mm i.d. and 115 mm in length. The catalytic reactor was situated within a Shimadzu 14-A gas chromatograph, in the oven that was designed for a commercial on-column OCI–14 injector. It was possible to temperature programme the reactor oven independently from the other heated sections of the gas chromatograph. The Pt/Al_2O_3 catalysts were placed in the middle of reactor, housed on a quartz wool holder, with thermocouples on the top and bottom of the catalyst bed. The reactor was loaded with 0.1 g of granulated Pt/Al_2O_3 catalysts, corresponding to a volume of 0.135 cm^3. In order to load the integral reactor, the whole catalysts spheres were completely homogeneously crushed down to 0.05 mm and pelletised. The tablets were ground and various granulations of catalyst were separated. The applied air flow rates through the catalyst bed corresponded to a space velocity of 17,500 h^{-1}. The investigated temperature range was between 110 and 140 °C. The temperatures were maintained with an accuracy of ±0.2 °C. The kinetics measurements were performed under steady state conditions and at a conversion of DMA below 10%, to ensure the validity of the differential reactor assumption. Although, the range of conversion under 10% could be *a priori* accepted as kinetic, i.e., the region in which the surface reaction is the rate determining step of the overall process, the absence of an internal diffusion limitation was confirmed by using different granulations of catalyst. There were no significant differences between the conversions obtained with catalyst particles of mean diameter below 0.5 mm, in investigated temperature range. Based on these tests, the kinetic study was performed with catalysts particles of 0.25 mm mean diameter. The dependence of the reaction rate on the hydrocarbon concentration was measured by varying the concentration of DMA in the air (range from 50 to 2600 ppm). Measurements of the inlet and outlet concentrations of DMA were performed using an FID detector. The DMA concentrations were determined with an accuracy of ±2 ppm. The reproducibility of the results was verified by performing each test several times. The reaction rates are expressed as the turnover frequency (TOF), defined as the number of the molecules reacting per second per one exposed Pt atom.

3. Results and discussion

Knowledge of the adsorption stoichiometry is necessary for the analysis of the CO chemisorption data and determination of the Pt mean crystallite size. It is well known that CO can form linear or bridged bonds with surface Pt atoms. The ratio of linear to bridged bonds depends on the size and structure of the Pt particles [23] and on the nature of the support. There are many studies that compare CO chemisorption with H_2 chemisorption and TEM results. There is general agreement that in the case of high Pt dispersion, the CO/Pt adsorption stoichiometry is 1 [24–27]. However, as the Pt dispersion decreased, the stoichiometry between adsorbed CO and Pt can be changed. With decreasing Pt dispersion below 30%, literature data show that the CO/Pt adsorption stoichiometry is in the range from 1 to 0.5 [26–31].

Therefore, a CO/Pt adsorption stoichiometry of 1 was adopted for the calculations of Pt crystallite size for the highly dispersed Pt catalyst. However, for the sintered catalyst, the CO chemisorption data were analysed using the two limiting values of the chemisorption stoichiometry: CO/Pt of 1 (CO adsorbs on Pt via linear bonds only) and CO/Pt of 0.5 (two surface Pt atoms are bonded to the same CO molecule). The mean crystallite size of Pt was calculated with the assumption that Pt crystallites were cubic-shaped with one face in contact with the alumina surface. The calculated size of the Pt crystallites was 1 nm for the catalyst with

the high Pt dispersion (D = 86%), while, the catalysts with lower Pt dispersions (D from 5 to 11%) were considered as catalysts with crystallite sizes within the range from 15.5 to 7.8 nm. This range covers all ratios between the two CO-Pt bond types, bridged and linear bonds, which could co-exist at the surface.

To determine if there was any influence of the Pt crystallites size on the oxidation activity of the Pt/Al_2O_3 catalysts, the conversions of DMA deep oxidation were measured. The measurements were performed at a constant inlet concentration of DMA of 1700 ppm in air, with a space velocity of 17 500 h^{-1}. The temperature dependence of DMA conversion for Pt/Al_2O_3 catalysts with different mean Pt crystallites size, small and large, is shown in Fig. 1a.

The overall activities reflected in the S curves include different reaction regimes along the curves. Focusing attention on the kinetic region only, a decrease of the conversion on the larger Pt crystallites can be observed. For easier visualization, the same data up to 10% DMA conversions are shown in Fig. 1b.

Both catalysts attained a conversion of 90% at about 300 °C (Fig. 1a). Above this temperature, the activities of both catalysts were identical; indicating that the reaction is governed by external diffusion, i.e., mass transfer to the catalyst surface is the rate controlling step. The catalyst with the small Pt crystallites showed a slightly better light-off characteristic than the catalyst with the larger Pt crystallites. Bearing in mind that the catalyst with the larger Pt crystallites had a significantly lower number of exposed Pt

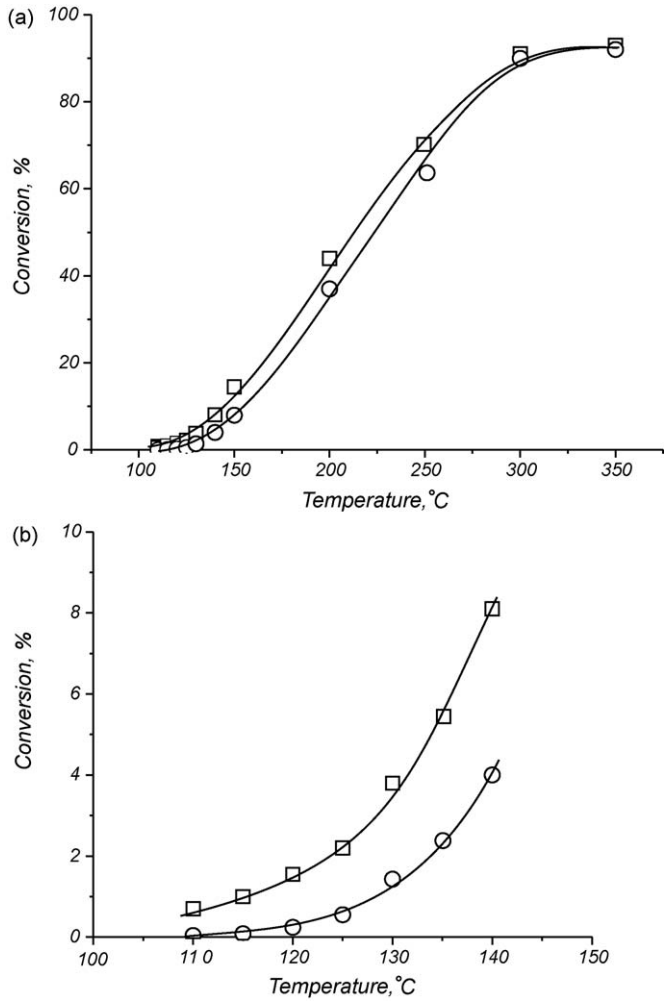

Fig. 1. Conversion of DMA (a) in the temperature range 100–350 °C; (b) up to 140 °C. Symbols: □-small Pt crystallite (d_{Pt}-1.0 nm); ○-large Pt crystallite (d_{Pt} 15.5 or 7.8 nm).

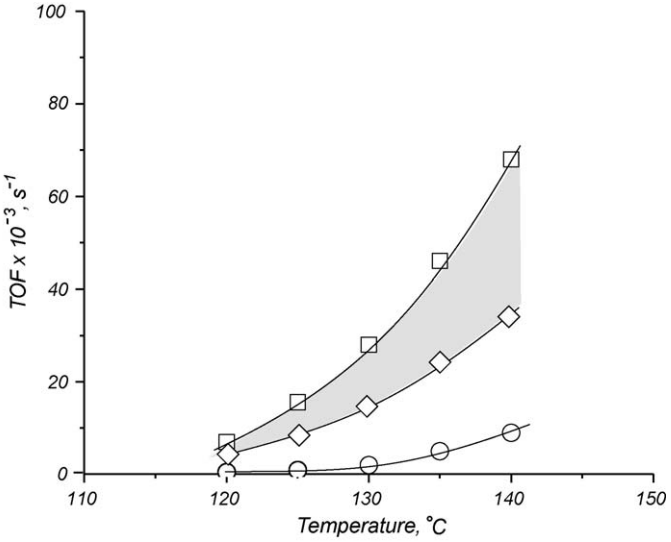

Fig. 2. The dependence of the TOF values in the kinetic region on temperature. Symbols: □, ◇- large Pt crystallite (d_{Pt} 15.5 or 7.8 nm, respectively); ○- small Pt crystallite (d_{Pt} 1.0 nm).

atoms than the catalyst with the small Pt crystallites, more pronounced differences in their activities could be expected. Therefore, it seems that some kind of compensation activity exists for the catalyst with the large Pt crystallites. This is clearly observable in Fig. 2, in which the TOF values for DMA oxidation are presented as a function of temperature. The TOF values for the large crystallites were calculated for two marginal values of the Pt crystallites size. The TOF values were calculated from the conversion data presented in Fig. 1b.

The shaded area for the TOF values of the large Pt crystallites (Fig. 2) contains all CO/Pt adsorption stoichiometry ratios between 0.5 and 1. The higher TOF values on the larger Pt crystallites than those on the small Pt crystallites suggest that DMA deep oxidation over Pt/Al_2O_3 catalysts is a structure sensitive reaction. The differences in TOF values on both Pt crystallite sizes retained the same ratio (≈5 or 10, depending on the accepted CO/Pt stoichiometry) over the whole investigated temperature range. To the best of our knowledge, this is the first study to demonstrate structure sensitivity for the reaction under investigation.

In order to provide an insight into the possible rate-determining elementary processes at the surface which are responsible for the structure sensitivity, a study of the kinetics of the complete oxidation of DMA as a function of temperature over a wide range of DMA concentrations over both the Pt/Al_2O_3 catalysts was conducted.

The TOF values as a function of DMA concentration obtained at different temperatures for both samples are presented in Figs. 3 and 4 for the small and large Pt crystallites, respectively. It should be noted that the TOF values for the large Pt crystallites (Fig. 4) are presented only for a CO/Pt adsorption stoichiometry of 1. The presentation of the other limiting CO/Pt stoichiometry (0.5) was omitted due to the same kinetic behaviour; only the TOF values were lowered by a factor 2.

The reaction pseudo-orders on both Pt/Al_2O_3 catalysts were determined by considering a power-law rate equation for TOF:

$$\mathrm{TOF} = k(C_{\mathrm{DMA}})^m(C_{\mathrm{O}})^n$$

where k is the apparent rate constant, C_{DMA} is the concentration of dimethylamine and C_O is the oxygen concentration. The symbols m and n represent the pseudo-orders with respect to DMA and oxygen, respectively. Since the molar ratio O_2/DMA was in the

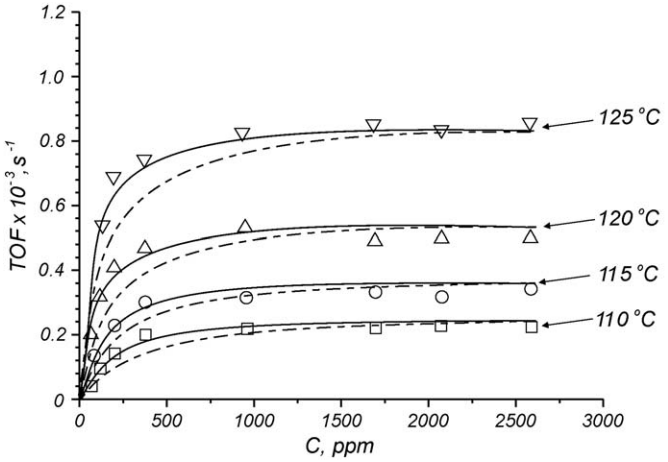

Fig. 3. TOF of DMA oxidation on Pt/Al_2O_3 catalyst with d_{Pt} 1.0 nm as a function of DMA concentration; Symbols: experimental data. Dashed lines: Mars van Krevelen model; Filled lines: Model based on the adsorption of the reactants on different active sites.

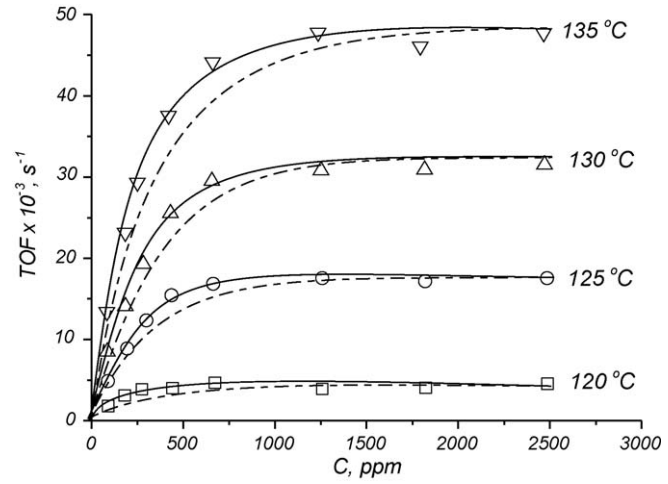

Fig. 4. TOF of DMA oxidation on Pt/Al_2O_3 catalyst with d_{Pt} 15.5 nm as a function of DMA concentration; Symbols: experimental data. Dashed lines: Mars van Krevelen model; Filled lines: Model based on the adsorption of the reactants on different active sites.

range from 80 to 4200, zero reaction order with respect to oxygen was considered.

Figs. 3 and 4 show that the kinetic behaviour for DMA oxidation was similar on both catalysts. For both Pt crystallite sizes, at lower DMA concentrations (lower than 300 ppm), the reaction order with respect to DMA was close to 1. For DMA concentrations above 1000 ppm, the reaction shifted towards a zero order, while fractional reaction orders were evident in the concentration region 300–1000 ppm.

Kinetic results for DMA deep oxidation may be interpreted by a Mars van Krevelen (MVK) mechanism [32], although Vannice [33] in a recent paper performed a critical analysis of the Mars van Krevelen rate expression. Numerous recent studies accept the MVK model to describe the oxidation of hydrocarbons over Pt catalysts [9,11–14,19,34,35]. This mechanism was initially proposed for the partial oxidation of organic compounds over oxide catalysts. This kinetics model can be used to describe deep oxidation of organic compounds over Pt catalysts assuming an oxidative reductive cycle at the Pt surface. Thus, this mechanism can be presented by the following elementary steps:

$$R + \text{oxidized catalyst} \xrightarrow{k_i} \text{reduced catalyst} + \text{products} \quad (1)$$

$$O_2 + \text{reduced catalyst} \xrightarrow{k_o} \text{oxidized catalyst} \quad (2)$$

where k_i represent the surface reaction rate constant, k_o represent the rate constant of surface reoxidation and R is a hydrocarbon. The reduced catalyst denotes an oxygen adsorption site. The oxidized catalyst denotes catalyst sites with chemisorbed oxygen. The rate expression for the above reactions is:

$$r = \frac{k_i k_o C_i C_O}{k_o C_o + \gamma k_i C_i} \quad (3)$$

where r is the oxidation rate, γ is the stoichiometric coefficient of oxygen in the overall reaction, and C_i and C_O represents the concentration of hydrocarbon and oxygen, respectively.

The Mars van Krevelen mechanism for oxidation over Pt catalysts assumed non-equilibrium dissociative adsorption of oxygen, rather than the real oxidation of the surface. It should be mentioned that same oxygen reaction path can be described by the Eley Rideal kinetic model, which generally includes catalytic reactions between a reactant from the gas phase with another reactant adsorbed on a surface.

First and zero order with respect to the hydrocarbon can be obtained in two limiting cases. Namely, if $k_oC_o \gg \gamma k_iC_i$, then $r = k_iC_i$ and first order kinetics with respect to the hydrocarbon can be described. Zero order kinetics with respect to hydrocarbon can be obtained if $\gamma k_iC_i \gg k_oC_o$ and then $r = k_oC_o/\gamma$.

Therefore, the already mentioned limiting cases of the Mars van Krevelen model were used to evaluate the values of k_i and k_o from the experimental data. For both catalysts, the k_i values were determined from the first order reaction regarding DMA in the low concentration regime (<300 ppm). Since the reaction order with respect to DMA was zero on both catalysts at higher concentrations of DMA (>1000 ppm), the corresponding values of k_o were evaluated from the intercept on the y-axis.

The in this manner evaluated surface reaction rate constant k_i and oxygen chemisorption rate constant k_o for the catalysts with small and large Pt crystallite sizes are presented in Arrhenius form in Fig. 5. The kinetic parameters for the large Pt crystallites are related to both limiting CO/Pt adsorption stoichiometries. The activation energies and the pre-exponential factors for the surface reactions rate constant k_i and the oxygen adsorption rate constant k_o were evaluated from the corresponding Arrhenius plots and are summarized in Table 1.

It should be noted that for the sintered catalyst, both activation energies (surface reactions and oxygen adsorption) do not depend on the CO/Pt adsorption stoichiometry, which

Table 1
The kinetic parameters for DMA oxidation according to the Mars van Krevelen kinetic model.

Sample	CO/Pt [a]	d_{Pt} (nm)	k_o (s^{-1})	k_i (s^{-1})	γ [b]	R^2 [c]
1	1	1.0	$2.5 \times 10^{14}\exp[-123/RT]$	$5.1 \times 10^{15}\exp[-117.5/RT]$	4.25	0.998
2	1	15.5	$1.3 \times 10^{14}\exp[-108/RT]$	$2.9 \times 10^{16}\exp[-117/RT]$	4.25	0.997
	0.5	7.8	$6.4 \times 10^{13}\exp[-108/RT]$	$1.4 \times 10^{16}\exp[-117/RT]$	4.25	0.997

[a] CO/Pt adsorption stoichiometry.
[b] γ, stoichiometric coefficient.
[c] R, correlation coefficient.

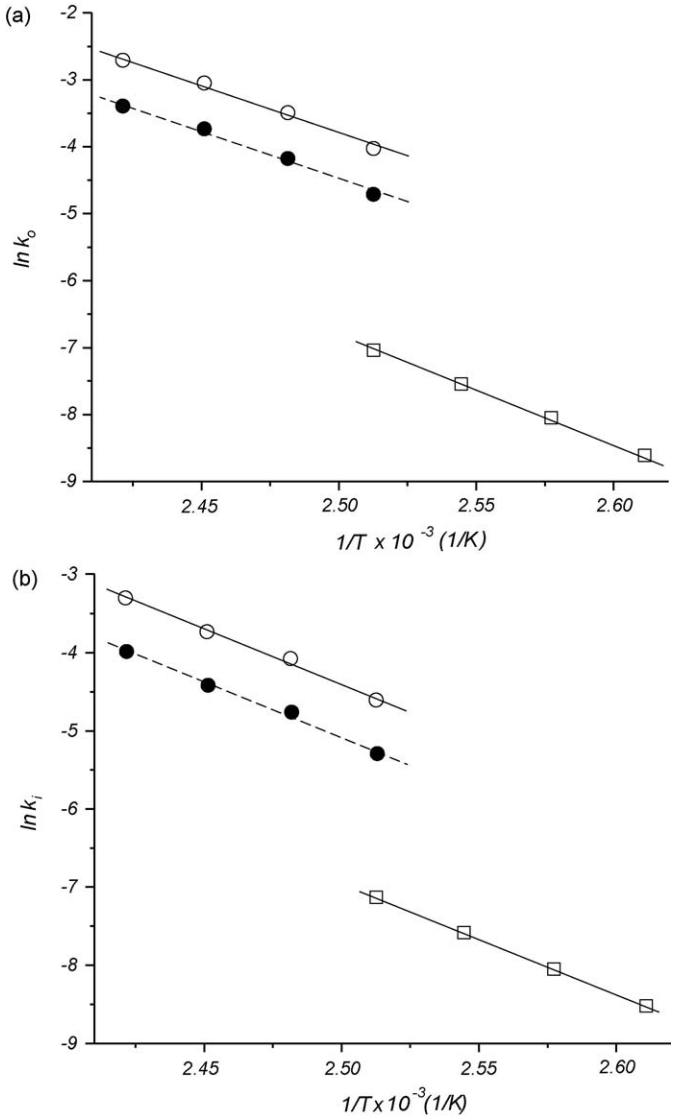

Fig. 5. Arrhenius plot for DMA oxidation on Pt/Al_2O_3 catalysts: (a) k_o; (b) k_i. Symbols: (□)- small Pt crystallite (d_{Pt} 1.0 nm); (○, ●)- large Pt crystallite (d_{Pt} 15.5 or 7.8 nm, respectively).

only affects the pre-exponential factor. The calculated kinetics parameters were applied in the Mars van Krevelen rate expression (Eq. (3)) to fit the experimental TOF data (dashed lines in Figs. 3 and 4). For both catalysts, in the range of the concentrations of DMA above 1500 ppm, the applied kinetic parameters fit the experimental data well, while at lower DMA concentrations, the model under predicts the experimental TOF values.

As can be seen from Table 1, the activation energy and pre-exponential factor of the oxygen chemisorption rate constant (k_o) obtained for the large Pt crystallites are considerably lower than for the small Pt crystallites. Moreover, these values are nearly identical with the activation energies and pre-exponential factors of k_o obtained for *n*-hexane and the toluene oxidation over the same catalysts [11,35]. These results are in accordance with the Mars van Krevelen model, which assumes that the oxygen chemisorption rate constant k_o should be independent of the type of oxidized hydrocarbons over the same catalyst. In other words, the rate of oxygen adsorption exclusively depends on the nature of the Pt active sites, i.e., depends on the Pt crystallite size, as presented in this study. The activation energy of the surface reaction (k_i) was approximately the same for both Pt crystallite sizes but the pre-exponential factor was higher for the catalyst with the large Pt crystallite size. Therefore, the surface reaction occurs via the same mechanism but the probability of the surface reaction is higher on the larger Pt crystallites. Consequently, the enhancement of the TOF at the large Pt crystallites should be assigned to the lower activation energy of oxygen adsorption on the reduced surface.

The obtained Mars van Krevelen kinetic parameters can be considered in terms of coordinative unsaturation of atoms on the different crystallite sizes. Namely, metal particles present on supported catalysts are non-uniform and may have a complex surface structure. These different types of surface atoms can have varying adsorption and reaction characteristics. The percent of corner and edge atoms and high energy sites decreases with increasing particle size. Assuming that Pt particles have a cubic metal shape, statistical calculation using the van Hardeveld and Hartog method [36] shows that the participation of edge atoms is tenfold higher for d_{Pt} = 1.0 nm than for d_{Pt} = 15.5 nm. Therefore, the increase in the activation energy of oxygen adsorption on the smaller Pt crystallites should be ascribed to the larger number of edge and corner sites. Oxygen is loosely held and more reactive on the larger Pt crystallites, causing an increase of the TOF values.

Also, the present kinetic results could be interpreted according to an oxidation model based on non-equilibrium adsorption of oxygen and adsorption of hydrocarbon on two different types of active sites. Mazzarino and Barresi [13] and Ordonez et al. [14] also employed this kinetic model. At this point, questions concerning the nature of these active sites arise.

First, the application of such assumptions is reasonable because crystallites of supported metal catalysts have surface atoms of different coordination (atoms on the corners, edges, planes, kinks). The portion of each of these types of surface atoms depends on the mean size of the crystallites.

Second, Delmon [37] suggested that the reacting zone in oxidation catalysis is much thicker and broader than the usual picture of adsorbed species on a perfectly located small spot, the active site. The reactants or reactant bound to catalysts interact with each other in a relatively thick layer near the surface, which can be indicated as the "boiling pot".

It is known that DMA, like every amine, is strongly adsorbed by Pt/Al_2O_3 catalysts [38] and the adsorption on Al_2O_3 mainly involves the formation of coordination bonds between the amine molecules and Lewis-acid surface sites [39,40]. Also, DMA adsorbs molecularly on a Pt surface through the lone pair electrons of its nitrogen, but the Pt surface promotes the decomposition of the adsorbed DMA towards very reactive intermediates [41].

In this case, XPS results [42] revealed that the $Pt4d_{5/2}$ binding energy for Pt/Al_2O_3 was shifted to a higher value (315.4 eV) as compared to metallic Pt (314.3 eV) reported in [43] for Pt/Al_2O_3 samples. This is attributed to the interaction of metallic Pt particles with the support due to charge transfer from the Pt to the electrophilic O^- species at the surface. Consequently, interaction with the support makes the platinum slightly positively charged, i.e., more liable to coordinate appropriate reactants. Probably, the Pt boundary sites ($Pt–Al_2O_3$) form different bonds with DMA in respect to Pt sites separated from the Al_2O_3 surface. Therefore, it might be assumed that $Pt–Al_2O_3$ boundary sites supply DMA to platinum.

Thus, the description of DMA deep oxidation over Pt/Al_2O_3 catalysts by this model is reasonable, assuming non-equilibrium adsorption of oxygen on one type of platinum site and reversible adsorption of DMA on another type of Pt site. The mechanism can

Table 2
The kinetic parameters for DMA oxidation according to the model based on the adsorption of the reactants on two different types of active sites.

Sample	CO/Pt [a]	d_{Pt} (nm)	k_o (s^{-1})	k_i (s^{-1})	K_H	γ [b]	R^2 [c]
1	1	1.0	$2.5 \times 10^{14} \exp[-123/RT]$	$1.7 \times 10^{15} \exp[-116.5/RT]$	1.52	4.25	0.999
2	1	15.5	$1.3 \times 10^{14} \exp[-108/RT]$	$2.1 \times 10^{16} \exp[-116/RT]$	1.46	4.25	0.998
	0.5	7.8	$6.4 \times 10^{13} \exp[-108/RT]$	$9.0 \times 10^{15} \exp[-116/RT]$	1.46	4.25	0.998

[a] CO/Pt adsorption stoichiometry.
[b] γ, stoichiometric coefficient.
[c] R, correlation coefficient.

be presented by the following elementary reaction steps:

$$O_2 + ()_O \xrightarrow{k_o} (O_2)_O \xrightarrow{()_O} 2(O)_O \quad (4)$$

$$R + ()_D \underset{k_{-1}}{\overset{k_1}{\rightleftarrows}} (R)_D \quad (5)$$

$$(O)_O + (R)_D \xrightarrow{k_i'} \text{Prod.} + ()_O + ()_D \quad (6)$$

where R represents DMA, k_1, k_{-1}, k'_i and k_o are the corresponding rate constants. $()_O$ denotes the platinum sites for oxygen adsorption and $()_D$ represent the active sites for DMA adsorption.

The following equation for the DMA oxidation rate (r) is obtained:

$$r = \frac{k_i' k_o K_H C_i C_o}{(1 + K_H C_i) k_o C_o + \gamma k_i' K_H C_i} \quad (7)$$

where C_i and C_o represent the concentration of hydrocarbon and oxygen, respectively. K_H (k_1/k_{-1}) is the adsorption constant of DMA.

Zero order kinetics with respect to the hydrocarbon can be obtained if $\gamma_i k/_i K_H C_i \gg k_o C_o$ and Eq. (7) becomes $r = k_o C_o/\gamma$. The values of k_o were determined in the same manner as for the Mars van Krevelen mechanism. The values of k'_i and Henry's constants were estimated to fit the experimental results presented in Figs. 3 and 4. In order to facilitate the fitting, the assumption that K_H is independent of temperature was adopted. The reaction constants were calculated iteratively according to Eq. (7). The kinetic parameters for DMA oxidation according to model based on the adsorption of reactants on different types of Pt active sites are presented in Table 2.

For both Pt crystallites size, as expected, the values of k_o obtained by this model were the same as the corresponding values obtained using the Mars van Krevelen model. Almost the same adsorption coefficient of close to 1.5 was evaluated to fit the values of the TOFs for both catalysts irrespective of the Pt crystallite size. The independence of Henry's adsorption coefficient from the Pt crystallite size suggests that DMA could be preferentially adsorbed on particular coordinated Pt sites, whether plane, edge, corner or kink Pt atoms. Another explanation could be that the adsorption of DMA occurs on interface Pt atoms (Pt–Al_2O_3), which might be considered identical, regardless of whether they are derived from small or large Pt crystallites.

Also, the evaluated surface reaction rate constants were almost the same as those obtained using the Mars van Krevelen mechanism. Thus, the oxidation model based on non-equilibrium adsorption of oxygen and adsorption of hydrocarbon on the different active sites demonstrates excellent agreement between the experimental and calculated TOF data (filled lines in Figs. 3 and 4) over the whole studied temperature and DMA concentration ranges.

The values of the surface reaction rate constant calculated from both the above-mentioned kinetic models reveals that DMA reacted through the same mechanism whether they reacted from the gas phase or adsorbed. The kinetic parameter in both models that was significantly changed by the different Pt crystallite size was the rate constant of oxygen adsorption, justifying the previous assumption that the oxygen bond strength is most responsible for the structure sensitivity of DMA deep oxidation. The strong Pt–O bond on the small Pt crystallites and a weak Pt–O bond on the large Pt crystallites are implicitly reflected in the values of the oxidation reaction rate (TOF), which increases with decreasing Pt–O bond strength.

4. Conclusions

The deep oxidation of DMA over Pt/Al_2O_3 catalysts is a structure sensitive reaction. The turnover frequency is higher for large than for small Pt crystallites. Two kinetic models were used to interpret the obtained results, i.e., the Mars van Krevelen mechanism and a mechanism based on the non-equilibrium adsorption of oxygen and adsorption of DMA on two different types of active sites.

The Mars van Krevelen model fits the TOF values very well at concentration of DMA higher than 1500 ppm, while in the lower concentration region, the model under predicts the experimental data. The model based on the adsorption of oxygen and DMA on different active sites fits the experimental data quite well over the whole studied temperature and concentration ranges. The fitted values for the Henry's adsorption constant are independent of Pt crystallite size.

The changes in the reactivity of oxygen on different Pt crystallite sizes can explain the structure sensitivity found for DMA deep oxidation. On large Pt crystallites, the oxygen involved in the surface reaction is loosely bound, enhancing the reactivity in the total oxidation of DMA. Moreover, the activation energy for the rate constant of oxygen adsorption is almost equal to those in the oxidation of *n*-hexane and toluene over the same catalysts [11]. These results support both the investigated models, showing that the rate constant of oxygen adsorption for the same Pt crystallite size is independent of the type of to be oxidised hydrocarbon.

Acknowledgement

This study was supported by the Ministry of Science and Environmental Protection of the Republic of Serbia (Proj. No. 142014G).

References

[1] J. Spivey, Ind. Eng. Chem. Res. 26 (1987) 2165.
[2] H. Chu, H. Widrawi, Chem. Eng. Prog. 92 (1996) 37.
[3] M. Boudart, Adv. Catal. 20 (1969) 153.
[4] L. Carballo, E. Wolf, J. Catal. 73 (1978) 366.
[5] M. Kobayashi, T. Kanno, A. Konishi, H. Takeda, React. Kinet. Catal. Lett. 37 (1988) 89.
[6] V. Labalme, E. Garbowsky, N. Ghilhaume, M. Primet, Appl. Catal. A: Gen. 138 (1996) 93.
[7] C. Pliangos, I.V. Yentekakis, V.G. Papadakis, C.G. Vayenas, X.E. Verykios, Appl. Catal. B: Environ. 14 (1997) 161.
[8] P. Papaefthimiou, T. Ioannides, X.E. Verykios, Appl. Catal. B: Environ. 15 (1998) 75.
[9] T.F. Garetto, C.R. Apesteguia, Catal. Today 62 (2000) 189.
[10] P. Marécot, A. Fakche, B. Kellali, G. Mabilon, M. Prigent, J. Barbier, Appl. Catal. B: Environ. 3 (1994) 283.
[11] N. Radic, B. Grbic, A. Terlecki-Baricevic, Appl. Catal. B: Environ. 50 (2004) 153.
[12] S. Gangwal, M. Mullins, J. Spivey, P. Caffrey, B. Tichenor, Appl. Catal. 36 (1988) 231.
[13] I. Mazzarino, A.A. Barresi, Catal. Today 17 (1993) 335.

[14] S. Ordonez, L. Bello, H. Sastre, R. Rosal, F. Diez, Appl. Catal. B: Environ. 38 (2002) 139.
[15] J. Gland, G. Sexton, B. Fisher, Surf. Sci. 95 (1980) 587.
[16] H. Wang, R. Tobin, D. Lambert, C. DiMaggio, G. Fisher, Surf. Sci. 372 (1997) 267.
[17] J. Gland, V. Korchak, Surf. Sci. 75 (1978) 733.
[18] P. Briot, A. Auroux, D. Jones, M. Primet, Appl. Catal. 59 (1990) 141.
[19] T. Garetto, C. Apesteguía, Appl. Catal. B: Environ. 32 (2001) 83.
[20] A. O'Malley, B.K. Hodnett, Catal. Today 54 (1999) 31.
[21] R. Hicks, H. Qi, M. Young, R. Lee, J. Catal. 122 (1990) 280.
[22] B. Grbic, N. Radic, A. Terlecki-Baricevic, Sci. Sinter 30 (1998) 179.
[23] S. Ladas, Surf. Sci. 175 (1986) L681.
[24] S. Wanke, P. Flynn, Catal. Rev. Sci. Eng. 12 (1975) 93.
[25] J.W. Bae, I.G. Kim, J.S. Lee, K.H. Lee, E.J. Jang, Appl. Catal. A: Gen. 240 (2003) 129.
[26] B. Ioan, A. Miyazaki, K. Aika, Appl. Catal. B: Environ. 59 (2005) 71.
[27] A.R. Vaccaro, G. Mul, J. Pérez-Ramírez, J.A. Moulijn, Appl. Catal. B: Environ. 46 (2003) 687.
[28] N. Job, M.F.R. Pereira, S. Lambert, A. Cabiac, G. Delahay, J.-F. Colomer, J. Marien, J.L. Figueiredo, J.-P. Pirard, J. Catal. 240 (2006) 160.
[29] J. Dawody, L. Eurenius, H. Abdulhamid, M. Skoglundh, E. Olsson, E. Fridell, Appl. Catal. A: Gen. 296 (2005) 157.
[30] J. Andersson, M. Antonsson, L. Eurenius, E. Olsson, M. Skoglundh, Appl. Catal. B: Environ. 72 (2007) 71.
[31] R. Ubago-Pérez, F. Carrasco-Marín, C. Moreno-Castilla, Appl. Catal. A: Gen. 275 (2004) 119.
[32] P. Mars, D.W. van Krevelen, Chem. Eng. Sci. 3 (1954) 41.
[33] M.A. Vannice, Catal. Today 123 (2007) 18.
[34] A.A. Barresi, G. Baldi, Chem. Eng. Sci. 47 (1992) 1943.
[35] B. Grbic, N. Radic, A. Terlecki-Baricevic, Appl. Catal. B: Environ. 50 (2004) 161.
[36] R. van Hardeveld, F. Hartog, Surf. Sci. 15 (1969) 189.
[37] B. Delmon, Catal. Today 117 (2006) 69.
[38] M. Arai, Y. Takada, T. Ebina, M. Shirai, Appl. Catal. A: Gen. 183 (1999) 365.
[39] J. Koubek, J. Volf, J. Pasek, J. Catal. 38 (1975) 385.
[40] J. Sokoll, H. Hobert, I. Schmuck, J. Catal. 121 (1990) 153.
[41] D.H. Kang, M. Trenary, Surf. Sci. 519 (2002) 40.
[42] B. Grbic, N. Radic, B. Markovic, P. Stefanov, D. Stoychev, Ts. Marinova, Appl. Catal. B: Environ. 64 (2006) 51.
[43] T. Ruhle, H. Schneider, J. Find, D. Herein, N. Pfander, U. Wild, R. Schlogl, D. Nachtingall, S. Artelt, U. Heinrich, Appl. Catal. B: Environ. 14 (1997) 69.